Angewandte Chemie
Eine Zeitschrift der Gesellschaft Deutscher Chemiker

Supporting Information

© Wiley-VCH 2013

69451 Weinheim, Germany

Intrinsic Allosteric Inhibition of Signaling Proteins by Targeting Rare Interaction States Detected by High-Pressure NMR Spectroscopy**

Hans Robert Kalbitzer, Ina C. Rosnizeck, Claudia E. Munte, Sunilkumar Puthenpurackal Narayanan, Veronika Kropf, and Michael Spoerner*

anie_201305741_sm_miscellaneous_information.pdf

Supporting Information

Supporting Information

Table of contents:

1. Experimental Procedures

2. Supplementary Figures

3. Complete references of main article

1. Experimental Procedures

1.1 Materials

Protein purification and sample preparation. Wild-type and mutants of Ras(1-166) were expressed in *Escherichia coli* strain BL21 and purified as described before.[1] Nucleotide exchange to GppNHp was performed as described by ref. [2]. Uniform ^{15}N isotope enrichment was performed by using the new minimal medium[3] containing 1 g/L $^{15}NH_4Cl$. Free nucleotides and phosphates were removed by gel filtration. The final purity of the protein was >95% as judged by SDS polyacrylamide gel electrophoresis. The samples contained 1.05 mM (278 K) and 1.84 mM (303 K) ^{15}N-labeled Ras(wt)·Mg^{2+}·GppNHp in 40 mM Tris/HCl, pH 7.4, 10 mM $MgCl_2$, 2 mM DTE, 0.1 mM DSS, and 12% D_2O.

1.2 Methods

Data collection. High-pressure NMR spectra were recorded with a Bruker Avance-800 NMR spectrometer equipped with a 5 mm TCI cryoprobe operating at ^1H and ^{15}N resonance frequencies of 800.12 and 81.08 MHz, respectively. High-pressure NMR spectroscopy was performed with an one-line high pressure system[4] developed in our laboratory.[5] Pressure is produced either by a home-built manual pressure bench or a spectrometer controlled high pressure pump (HUP440, Pressure BioSciences Inc, South Easton, MA). Either a quartz capillary with an outer diameter of 4 mm and an inner diameter of 1.2 mm or a ceramic cell with an outer diameter of 4 mm and an inner diameter of 1.1 mm was used. Special care was taken to protect the cryoprobe from damage by using a special autoclave system.[6]

At every pressure step a phase-sensitive [^1H,^{15}N]-HSQC experiment was performed. Each 2D spectrum was recorded as a complex data matrix comprised of 2048 x 512 points using a spectral width of 8400 Hz in the ^1H-dimension and 2400 Hz in the ^{15}N-dimension. A recycle delay of 3.4 s was used with 8 scans/FID and 16 scans/FID for the sets of 2D-spectra performed at 278 K and 303 K, respectively. At 278 K additional experiments with 32 scans/FID have been recorded at 3 MPa and 200 MPa. Before and after each 2D experiment a standard ^1H NMR spectrum was recorded. ^1H chemical shifts were directly and ^{15}N chemical shifts were indirectly referenced to DSS using a Ξ-value 10.1329118.[7] The absolute temperature inside the probe head was

calibrated by measuring the chemical shift difference $\Delta\delta$ between the methyl and hydroxyl resonance of 100% methanol.[8]

Data Processing and Evaluation. The assignment of the amide resonances for Ras(wt)·Mg^{2+}·GppNHp was taken from *Ito et al.*.[9] They were adapted to our pH and temperature conditions by performing a temperature and pH series starting with the conditions used by the authors (pH 5.5, 310 K). All NMR spectra were processed using TOPSPIN 2.0 (BrukerBioSpin, Karlsruhe). Data analysis was performed using the AUREMOL software.[10]

Analysis of the Chemical Shifts. The pressure dependence of the chemical shifts δ of the amide protons and nitrogen atoms in the [^{1}H, ^{15}N]-HSQC spectra of the protein was first corrected for unspecific effects by subtracting the known pressure dependence of chemical shifts of the random-coil peptides Ac-Gly-Gly-X-Ala-NH_2 from the experimental data.[11] Two different expressions were used for a fit of the obtained chemical shifts δ^* as function of pressure p, as a model-free approximation the second order Taylor expansion

$$\delta^*(p,T_0) \approx \delta_0^*(p_0,T_0) + B_1^*(p-p_0) + B_2^*(p-p_0)^2 \qquad (1)$$

and/or the thermodynamical N-site exchange model. In equation (1) δ^*_0 is the chemical shift at ambient pressure $p_{0,}$ and B^*_1 and B^*_2 are the first and second order pressure coefficients. The magnitude of the pressure coefficients depends on the magnitude of the local structural changes induced by pressure and thus can be used as a semi quantitative measure for these changes. If there is an equilibrium between M states i, (i=1,N) of the protein, under fast exchange conditions ($|\Delta\omega_{ij}| = |\omega_j - \omega_i| << 1/\tau_{ex}$, with τ_{ex} the exchange correlation time) the observed chemical shift is a combination of the chemical shifts δ_i of each state. It can be described as

$$\delta = \frac{\sum_{i=1}^{M} \delta_i e^{-\frac{\Delta G_{1i}}{RT}}}{\sum_{i=1}^{M} e^{-\frac{\Delta G_{1i}}{RT}}} \quad . \qquad (2)$$

The Gibbs free energy ΔG_{1i} is given[12] as

$$\Delta G_{1i}(T_0, p) = \Delta G^0_{1i}(T_0, p_0) + \Delta V^0_{1i}(p - p_0) - \frac{\Delta \beta^{0\prime}_{1i}}{2}(p - p_0)^2 \qquad (3)$$

where ΔV^0_{1i} and $\Delta \beta^{0'}_{1i}$ are the differences of the partial molar volumes and of the partial molar compressibility factors between states 1 and i at temperature T_0 and pressure p_0, respectively. For the calculations of the ΔG_{ij} values the quadratic term in equation (3) has been neglected in this paper.When in addition N-M states are in slow exchange, equation (2) still describes the conformational ensemble.

Analysis of the Signal Volumes. Quantification of NMR-visible resonances was performed by using the integrals of the corresponding methylene resonances of Tris/HCl added to the sample with a known concentration.The normalized change of the cross peak volume $\Delta V_i(p)/V(p_0)$ in the HSQC spectrum is given by

$$\frac{\Delta V_i(p)}{V_i(p_0)} = \frac{V_i(p)}{V_i(p_0)} - 1 = \frac{c_T(p)}{c_T(p_0)} f_i(p) - 1 \quad , \qquad (4)$$

with c_T the total concentration of the protein. The function f_i depends on the physical process influencing the individual cross peak intensities. The reduction of the corrected cross peak volumes can be due (1) to T_2-processes that make the INEPT-transfer less effective, (2) to the transfer of saturation from the water protons exchanging with the amide protons and/or (3) to slow exchange between (at least) two states. Since only minor line broadening is observed with pressure the first mechanism can be ruled out. Since presaturation of the water signal also has no significant effect on the observed pressure dependence, the second effect can be neglected. In case of slow exchange (3) a second set of additional cross peaks would be expected corresponding to a second state of the peptide. Only a limited number of new cross peaks can be

identified and assigned. This may be due to overlap with other peaks in the spectrum as well as to additional broadening of the new cross peaks. An important line broadening mechanism for the additional amide resonances would be the exchange with the bulk water as it is usually observed for random-coil structures at pH 7.4.

When the conformational exchange between the states *i* and *j* is slow relative to the time scale of the NMR experiment ($|\Delta\omega_{ij}| >> 1/\tau_{ex}$), the signal volume V_i of state *i* is proportional to its concentration c_i. The equilibrium constant K_{ji} can be calculated from the cross-peak volumes *V* of the HSQC spectra by

$$K_{ji} = \frac{V_i}{V_j} = e^{-\frac{\Delta G_{ji}}{RT}} \qquad (5)$$

If only one peak $j = 1$ can be observed then V_1 is given by

$$V_1(p) = \frac{V_T(p)}{\sum_{i=1}^{N} e^{-\frac{\Delta G_{1i}(p)}{RT}}} \qquad (6)$$

With V_T(p) the total cross peak volume corresponding to the sum of all states at pressure *p*. When the volume *V* of the observed peak is derived from M states 1,..,M in fast exchange, equation (6) can be generalized to

$$V(p) = \frac{V_T(p)\sum_{i=1}^{M} e^{-\frac{\Delta G_{1i}(p)}{RT}}}{\sum_{i=1}^{N} e^{-\frac{\Delta G_{1i}(p)}{RT}}} \qquad (7)$$

When the protein concentration remains constant $V_T(p)$ can be replaced by $V_T(p_0)$ and $f_1(p)$ is given by

$$f_1(p) = \frac{\sum_{i=1}^{M} e^{-\frac{\Delta G_{1i}(p)}{RT}} \sum_{i=1}^{N} e^{-\frac{\Delta G_{1i}(p_0)}{RT}}}{\sum_{i=1}^{N} e^{-\frac{\Delta G_{1i}(p)}{RT}} \sum_{i=1}^{M} e^{-\frac{\Delta G_{1i}(p_0)}{RT}}} \qquad (8)$$

For extracting the thermodynamic parameters from the pressure dependent HSQC spectra in a multi-state model, one can use the fact that some residues selectively detect a single transition since other transitions do not have a direct influence on the chemical shift and/or cross peak volumes. The obtained values can be used as first approximations for the corresponding parameters, when a number of residues can be assigned to a given transition they can be averaged and used for afirst error estimation. For getting reliable initial values primarily only signals should be evaluated that show significant pressure effects and clearly are due to a single transition. The obtained parameters for a given transition then can be refined using the values obtained for the other transitions on the basis of equations 2 and 8 (see also ref. [13]).

Relative populations in an *N*-state system.The relative population p_i can be calculated from the equilibrium constants K_{ij} = [j]/[i] as

$$p_i(p, T_0) = \frac{K_{1i}(p, T_0)}{\sum_{j=1}^{N} K_{1j}(p, T_0)} \quad , \qquad (9)$$

with 1 an arbitrarily selected state.

References

[1] J. Tucker, G. Sczakiel, J. Feuerstein, J. John, R. S. Goody, A. Wittinghofer, *EMBO J.* **1986**, *5*, 1351-1358.

[2] J. John, R. Sohmen, J. Feuerstein, R. Linke, A. Wittinghofer, R. S. Goody, *Biochemistry* **1990**, *29*, 6058-6065.

[3] N. Budisa, B. Steipe, P. Demange, C. Eckerskorn, J. Kellermann, R. Huber, *Eur. J. Biochem.***1995**, *230*, 788-796.

[4] T. Yamaguchi, H. Yamada, K. Akasaka, *J. Mol. Biol.* **1995**, *250*, 669-694.

[5] M. R. Arnold, H. R. Kalbitzer, W. Kremer, *J. Magn. Reson*. **2003**, *61*, 127-131.

[6] M. Beck Erlach, C. E. Munte, W. Kremer, R. Hartl, D. Rochelt, D. Niesner, H. R. Kalbitzer, *J. Magn. Reson.* **2010**, *204,* 196-199.

[7] D. S. Wishart, C. G. Bigam, J. Yao, F. Abildgaard, H. J. Dyson, E. Oldfield, J. L. Markley, B. D. Sykes, *J. Biomol. NMR* **1995**, *6*, 135-140.

[8] D. S. Raiford, C. L. Fisk, E. D. Becker *Anal. Chem.* **1979**, *51*, 2050-2051.

[9] Y. Ito, K. Yamasaki, J. Iwahara, T. Terada, A. Kamiya, M. Shirouzu, Y. Muto, G. Kawai, S. Yokoyama, E. D. Laue, M. Wälchli, T. Shibata, S. Nishimura, T. Miyazawa, *Biochemistry* **1997**, *36*, 9109-9119.

[10] W. Gronwald, H. R. Kalbitzer, *Progr. NMR Spectr.* **2004**, *44*, 33-96.

[11] J. Koehler, M. Beck Erlach, E. Crusca Jr., W. Kremer, C. E. Munte, H. R. Kalbitzer, Materials **2012**, *5*, 1774-1786.

[12] K. Heremans, L. Smeller, *Biochim. Biophys. Acta* **1998**, *1386*, 353-370.

[13] C. E. Munte, M. Beck Erlach, W. Kremer, J. Koehler, H. R. Kalbitzer, *Angew. Chem.* **2013**, *125*, 9111-9116; *Angew. Chem. Int. Ed.*, **2013**, *52*, 8943-8947.

[14] P. A. Boriak-Sjodin, S. M. Margarit, D. Bar-Sagi, J. Kuriyan, *Nature* **1998**, *394*, 337-343.

[15] I. Vetter, T. Linnemann, S. Wohlgemuth, M. Geyer, H. R. Kalbitzer, C. Herrmann, A. Wittinghofer, *FEBS Lett.* **1999**, *451*, 175-180.

[16] K. Scheffzek, M. R. Ahmadian, W. Kabsch, L. Wiesmüller, A. Lautwein, F. Schmitz, A. Wittinghofer, *Science* **1997**, *277*, 333-338.

[17] F. H. Schumann, H. Riepl, T. Maurer, W. Gronwald, K.-P. Neidig, H. R. Kalbitzer, *J. Biomol. NMR* **2007**, *39*, 275-289.

2. Supplementary figures

Figure S1

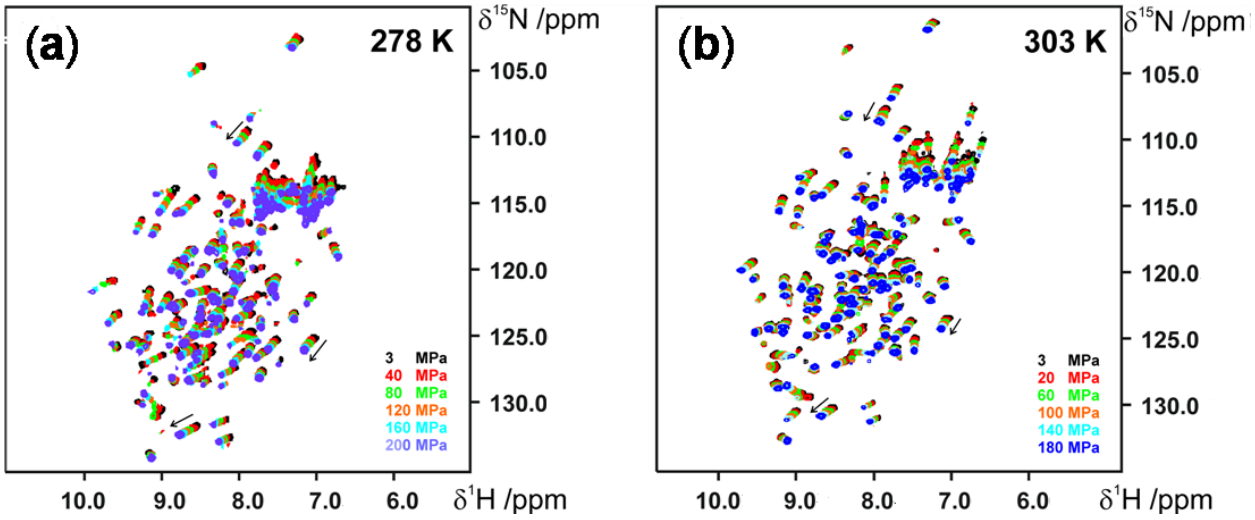

Figure S1: **[^{1}H, ^{15}N]-HSQC spectra of Ras(wt)·Mg^{2+}·GppNHp at different pressures.** Overlay of the [^{1}H, ^{15}N]-HSQC spectra of Ras(wt)·Mg^{2+}·GppNHp in 40 mM Tris/HCl, pH 7.4, 10 mM $MgCl_2$, 2 mM DTE, 0.1 mM DSS and 12% D_2O at different pressures. **(a)** Ras concentration 1.05 mM, T = 278 K, **(b)** Ras concentration 1.84 mM, T = 303 K. The direction of chemical shift with increasing pressure is indicated by the arrows. All spectra have been recorded at 800 MHz proton frequency.

Figure S2

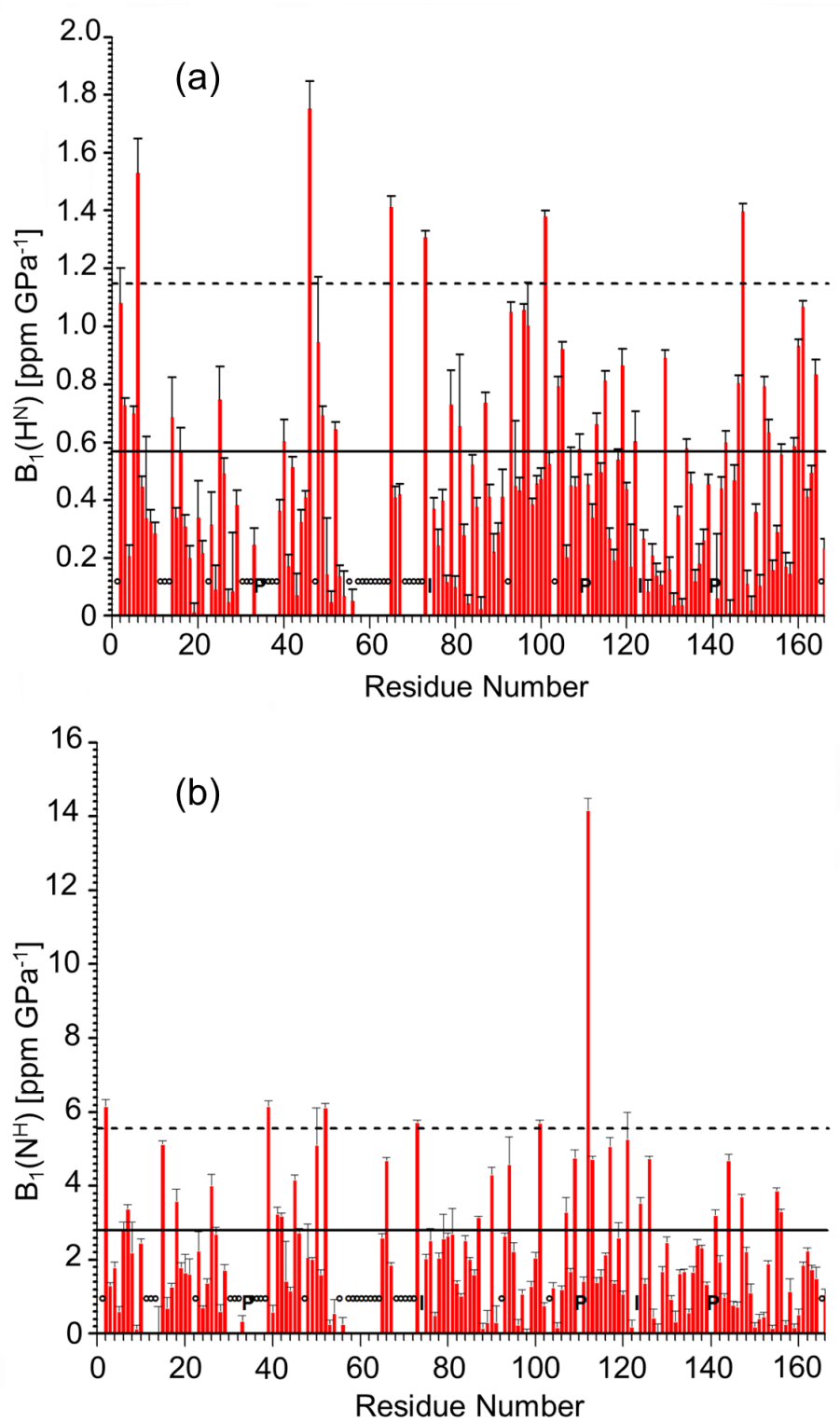
(a)
$B_1(H^N)$ [ppm GPa^{-1}]
Residue Number
(b)
$B_1(N^H)$ [ppm GPa^{-1}]
Residue Number

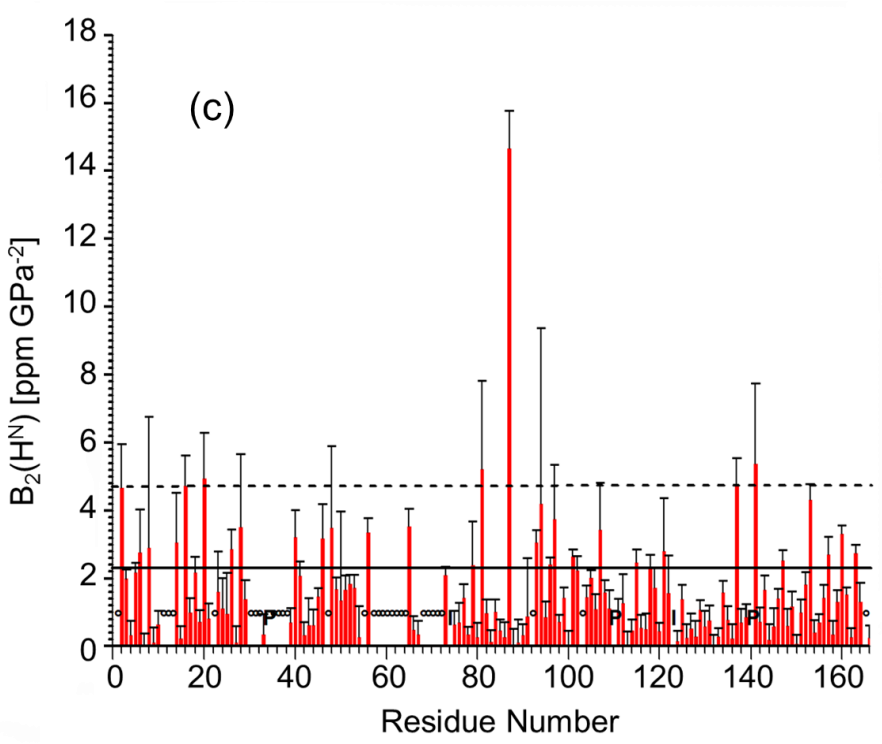
(c)
$B_2(H^N)$ [ppm GPa^{-2}]
Residue Number

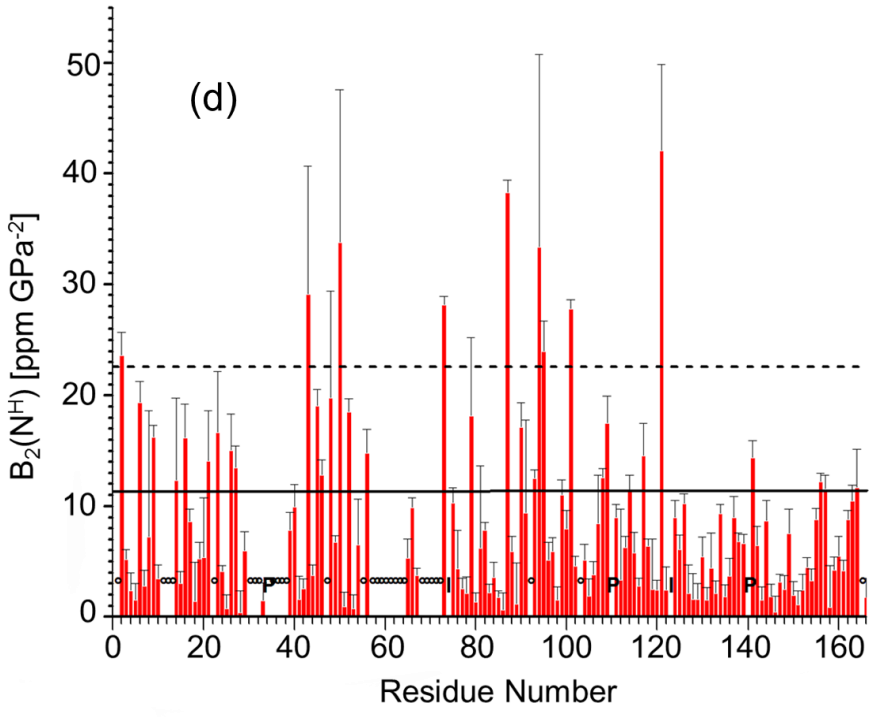
(d)
$B_2(N^H)$ [ppm GPa^{-2}]
Residue Number

Figure S2: **First order and second order pressure coefficients of wild type Ras·Mg^{2+}·GppNHp at 303 K.** Sample composition see Figure S1. Data were corrected for random coil effects before calculation of the pressure coefficients $B_{1,2}$*. Absolute values of the first order pressure coefficients B_1*(H^N) **(a)**, B_1*(N^H) **(b)**, B_2*(H^N) **(c)**, and B_2*(N^H) **(d)** as a function of the primary sequence. The standard deviation σ_0 to zero (solid line) and 2 σ_0 (dashed lines) are shown. Prolines are marked with (P), not assigned or not assignable residues with (o) and residues, for which the coefficients could not be determined due the loss of signal intensity within the pressure series, are marked with I.

Figure S3

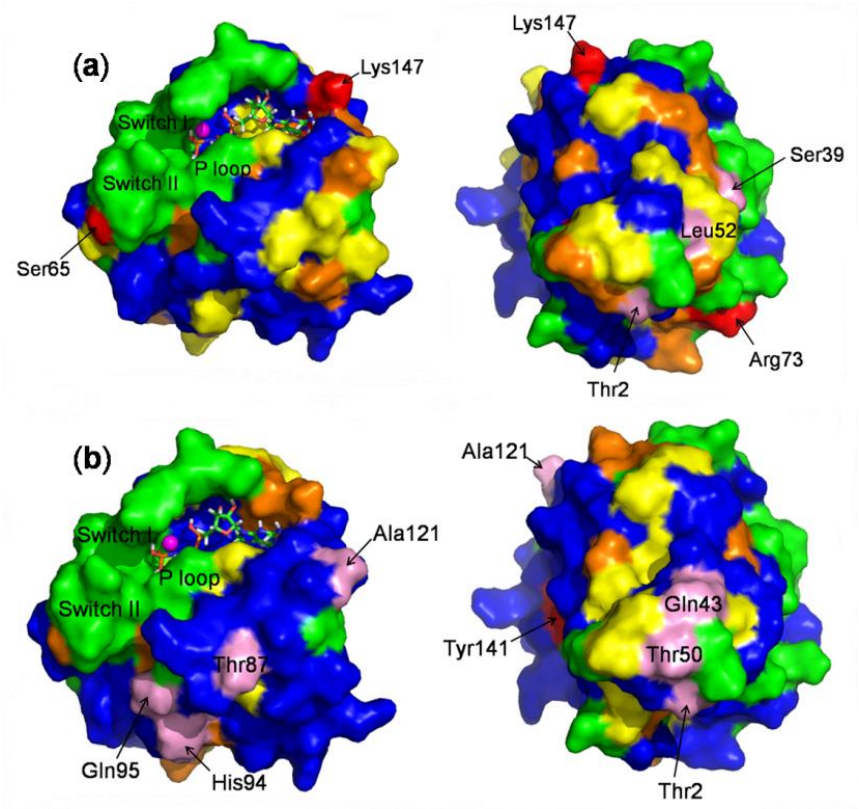

Figure S3: **Pressure induced chemical shift changes in Ras.** Data taken from Figure S2. Residues exhibiting significant large first **(a)** and second order **(b)** pressure coefficients for the amide protons and amide nitrogen atoms mapped onto the surface of the crystal structure of Ras(wt)·Mg^{2+}·GppNHp (pdb 5p21). **(a)** Residues with pressure coefficients B_1* in the interval $\sigma_0 < B_1^* \leq 2\ \sigma_0$ are depicted in orange for $^1H^N$ and yellow for $^{15}N^H$. Residues with $B_1^* > 2\ \sigma_0$ are depicted in red for $^1H^N$ and in pink for $^{15}N^H$. **(b)** Residues with pressure coefficients B_2 in the interval $\sigma_0 < B_2^* \leq 2\ \sigma_0$ are depicted in orange for $^1H^N$and yellow for $^{15}N^H$. Residues with $B_2^* > 2\ \sigma_0$ are depicted in red for $^1H^N$ and in pink for $^{15}N^H$. Amino acids, which are not visible in the [^{1}H, ^{15}N]-HSQC spectrum of Ras(wt)·Mg^{2+}·GppNHp or could not be followed within the pressure series are shown in green. Residues with $B_{1,2} \leq \sigma_0$ are colored blue.

Figure S4

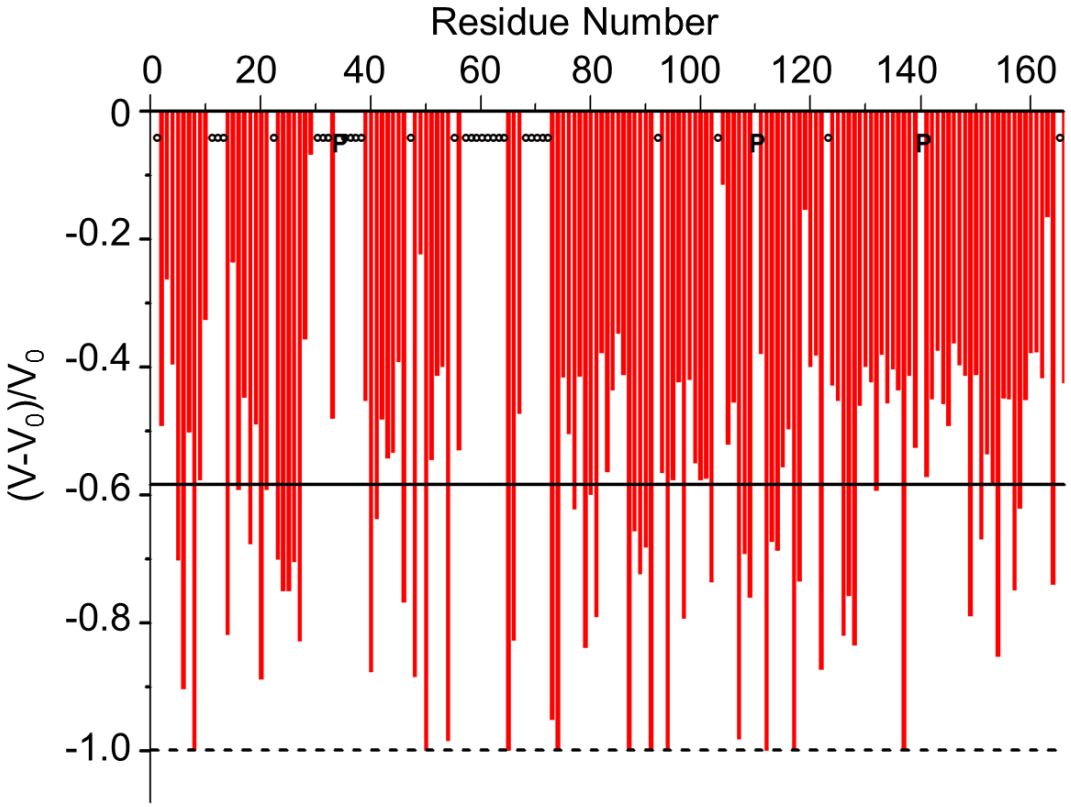

Figure S4: **Pressure induced cross peak volume changes.**The relative difference of the [^{1}H, ^{15}N]-HSQC cross-peak volumes V_0 measured at 3 MPa and V measured at 180 MPa plotted as a function of the amino acid sequence of Ras(wt)·Mg^{2+}·GppNHp at 303 K. Experimental conditions see Figure S1. The σ_0 value of the peak volume changes is shown by the solid line. Prolines are marked with (P), not assigned or not assignable residues, with (o) and residues, for which the coefficients could not be determined due the loss of signal intensity within the pressure series are marked with I.

Figure S5

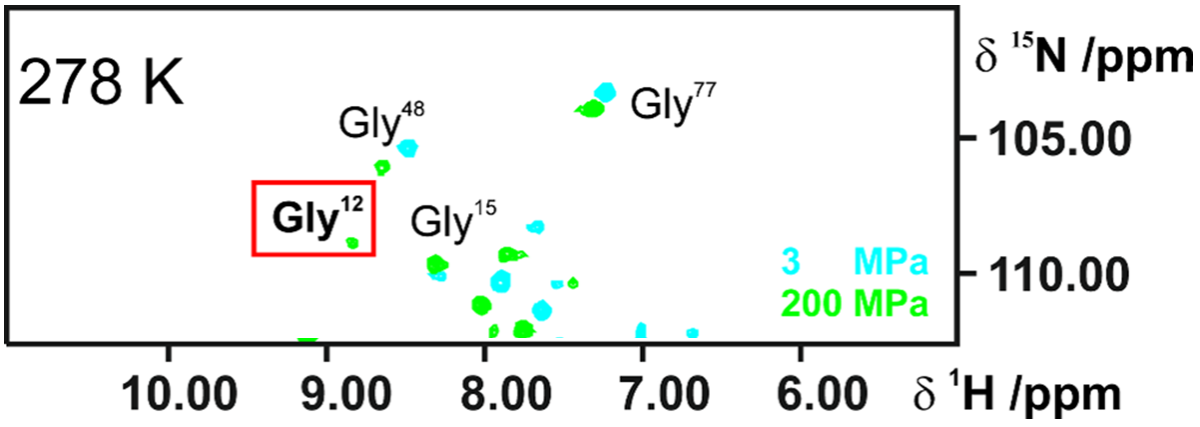

Figure S5: **Appearance of new cross peaks at high pressure.** Experimental conditions as in Figure S1. The signal of Gly12 that is only observable at high pressures is labeled by a red square.

Figure S6

Figure S6: **Sequence specific pressure effects and sequence motifs in H-Ras.** Green box, P-loop, PM1 motif (G10xxxxGKS17), red box, switch I (30-40), blue box, switch II (60-76), violet box, PM2 (T35), purple box PM3 (D57xxGQ), brown box, G1-motif (F28), teal box, G2-motif (N116KxD), dark yellow box, G3 motif, (S145AK147). **(a)** Residues, showing strong pressure effects. Residues with pressure coefficients $B_{1,2}^* < 2\ \sigma_0$ and at least one in the range of $\sigma_0 < B_1^* \leq 2\ \sigma_0$ are depicted in orange. Residues with at least one pressure coefficient $>2\ \sigma_0$ are depicted in red. **(b)** Residues involved in the C2-C1 transition are colored green, **(c)** residues involved in the C2-C3 transition are colored blue, **(d)** residues involved in the C2-C4 transition are colored purple, **(e)** residues directly involved in protein-protein interaction of Ras with Sos (pdb 1BKD),[14] RalGDS,[15] and Ras-GAP (pdb 1WQ1).[16] Interaction sites were calculated according to Schumann *et al.* 2007[1].[17] Sos only (dark yellow), RalGDS only (pink), GAP only (orange), Sos, GAP and RalGDS (aqua), Sos and GAP (purple), Sos and RalGDS (turquoise), RalGDS and GAP (dark red).

Figure S7

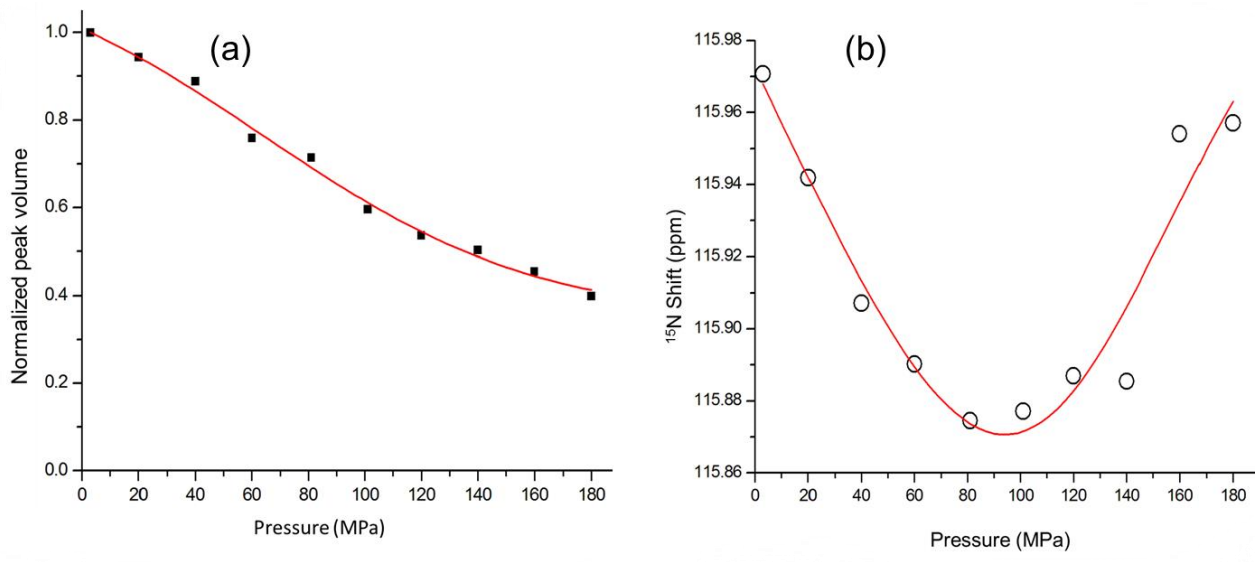

Figure S7: **Pressure induced spectral changes fitted with a thermodynamic model. (a, b)** Fit of the pressure dependent volume and $^{15}N^{H}$ chemical shift changes of amide cross peaks in an [^{1}H, ^{15}N]-HSQC spectrum of Ras(wt)·Mg^{2+}·GppNHp., T=303 K. **(a)** Glu49, fit of the data assuming slow exchange in a two state model with ΔG_{24} 12.36 kJ mol^{-1}, ΔV_{24} -115 mL mol^{-1} (χ^2 0.00026). **(b)** Gln95, fit with a three-state model assuming fast exchange in the NMR time scale with ΔG_{21} 1.48 kJ mol^{-1}, ΔV_{21} -18 mL mol^{-1}, ΔG_{23} 5.18 kJ mol^{-1}, ΔV_{23} -81 mL mol^{-1} (χ^2 0.00015).

Figure S8

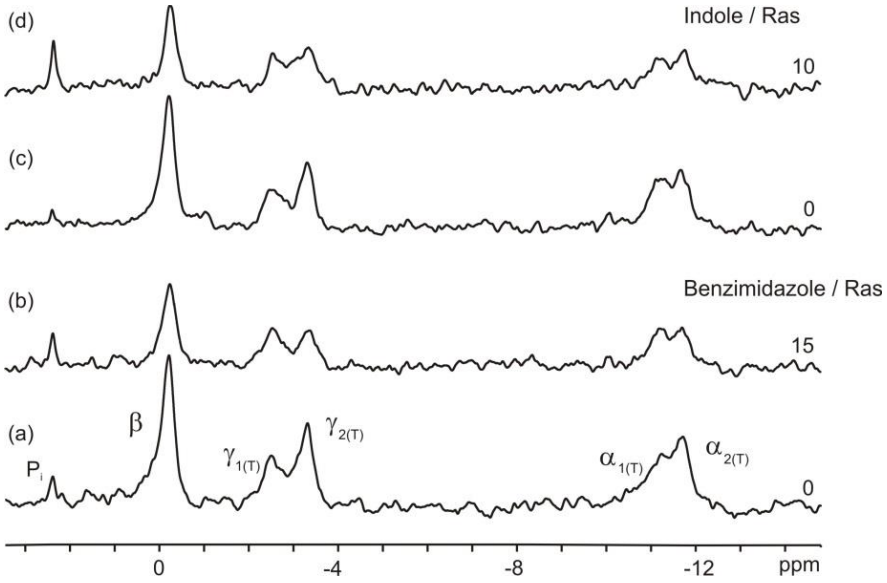

Figure S8: **Stabilization of state 1(T) by indole and benzimidazole.** ^{31}P NMR spectra of Ras(H166A)·Mg^{2+}·GppNHp in the absence and presence of indole and benzimidazole, respectively. T = 278 K. The mutant Ras(H166A)·Mg^{2+}·GppNHp has been used, since it has been shown earlier that mutation of the second Zn^{2+}-cyclen binding site at His166 does not has an effect on the conformational equilibrium but excludes possible artifacts by interaction of small compounds with the C-terminal histidine residue. (**a, b**) The sample contained 0.7 mM Ras(H166A)·Mg^{2+}·GppNHp in 40 mM Tris/HCl, 10 mM $MgCl_2$, 2 mM DTE, 0.2 mM DSS, 90% H_2O/10% D_2O, pH 7.4 in the absence (**a**) or presence (**b**) of 10.7 mM benzimidazole. (**c, d**) The sample contained 1.1 mM Ras(H166A)·Mg^{2+}·GppNHp in the above buffer in the absence (**c**) or presence (**d**) of 10 mM indole. As to be expected for a 1(T) inhibitor binding causes a shift from state 2(T) to 1(T).

3. Complete references from main article

[12] I. C. Rosnizeck , T. Graf, M. Spoerner, J. Tränkle, D. Filchtinski, C. Herrmann, L. Gremer, I. R. Vetter, A. Wittinghofer, B. König, H. R. Kalbitzer, *Angew. Chem*. **2010**, *122*, 3918-3922; *Angew. Chem. Int. Ed. Engl.* **2010**, *49*, 3830-3833.

[14] T. Maurer, L. S. Garrenton, A. Oh, K. Pitts, D. J. Anderson, N. J. Skelton, B. P. Fauber, B. Pan, S. Malek, D. Stokoe, M. J. Ludlam, K. K. Bowman, J. Wu, A. M. Giannetti, M. A. Starovasnik, I. Mellman, P. K. Jackson, J. Rudolph, W. Wang, G. Fang, *Proc. Natl. Acad. Sci. U.S.A.* **2012**, *109*, 5299-5304.

[17] Y. Ito, K. Yamasaki, J. Iwahara, T. Terada, A. Kamiya, M. Shirouzu, Y. Muto, G. Kawai, S. Yokoyama, E. D. Laue, M. Wälchli, T. Shibata, S. Nishimura, T. Miyazawa, *Biochemistry* **1997**, *36*, 9109-9119.